Analysis of consolidation behavior for saturated sand-marine clay mixtures considering the inter-granular structure evolution

By

Xiusong Shi

Department of Civil and Environmental Engineering

The Hong Kong Polytechnic University, Hong Kong, China

Email: xsshi@polyu.edu.hk

and

Jianhua Yin

Department of Civil and Environmental Engineering

The Hong Kong Polytechnic University, Hong Kong, China

Fax: (852) 2334-6389, Tel: (852) 2766-6065, Email: cejhyin@polyu.edu.hk

Manuscripts for submission to Journal of Engineering Mechanics, ASCE, for possible publication as an article.

May 2017

Abstract

Laboratory tests on sand-marine clay mixtures reveal that the effect of sand mass fraction on the overall consolidation behavior is negligible for a sand mass fraction of 20% or less. Further increase of the sand fraction significantly affects the overall consolidation process. To describe this behavior, a consolidation model is proposed within homogenization framework. The sand-marine clay mixture is divided into two systems: a clay matrix system consisting of the silts, clay particles and void space in the marine clay matrix, and an inclusion system consisting of sand particles. The volume fraction of sand particles is adopted as the structure variable, representing the inter-granular structure evolution of the sand-clay mixtures. Based on some reasonable assumptions, the governing equations are formulated and the consolidation problem is solved using Galerkin's weighted residual method within the finite element framework. The proposed consolidation model has five principal parameters: four intrinsic ones depending on the behavior of the pure clay matrix, and one structure parameter related to the inter-granular structure. Only two conventional oedometer tests are needed for the calibration of these model parameters. Comparison between the test data and the model prediction reveals that the model can well reproduce the effect of sand fraction on the overall consolidation behavior of the tested sand-marine clay mixtures.

Keywords: Consolidation; Sand-clay mixtures; Finite element method; Homogenization; Marine clay

Introduction

A sand-clay mixture is an important engineered material which is being used and produced in various projects. As a binary mixed material, it inherits some of the properties of the clay matrix and the sand inclusions. The overall permeability is lower than that of the granular material, and the compressibility is lower that of the pure clay due to the incompressible sand inclusions and their interactions. In some cases, the mentioned properties are favorable. E.g., due to the low permeability, it was adopted as engineered barriers to prevent the contaminants from a nuclear waste (Pusch and Gray 1989; Graham, *et al.*, 1992; Kenney *et al.*, 1992; Pandian *et al.*, 1995; de Magistris *et al.*, 1998; Sivapullaiah *et al.*, 2000). However, sometimes the low permeability is not desirable. The sand percolation effect induces sand-clay binary mixtures near the sand-clay interface in land reclamation (e.g., Tan *et al.*, 1994; Silva, 2016). The soft marine deposits are covered by the mixture layer (see Fig. 1) which acts as the drainage boundary of the underneath soft soil. Consequently, the consolidation process of the marine clay is coupled with that of the sand-marine clay mixture.

The behavior of sand-clay mixtures was documented by many researchers. Most of them focused on the permeability (Pandian *et al.*, 1995; Sivapullaiah *et al.*, 2000; Watabe *et al.*, 2011; Elkady *et al.*, 2015; Deng *et al.*, 2016) and compression behavior (Torfs, 1996; Kumar, 1996; Yin, 1999; Monkul *et al.*, 2005; Monkul and Ozden, 2007; Shi and Yin, 2017) based on element tests. In some previous work, the compressibility and permeability of sand-clay mixtures were estimated based on regression analysis (Yin, 1999; Sivapullaiah *et al.*, 2000; Deng *et al.*, 2016). Hence, the consolidation process of a sand-clay mixture can be reproduced using Terzaghi's consolidation theory by assuming a homogeneous soil element. However, this method doesnot consider the intergranular structure evolution with increasing sand fraction during consolidation process. A more reasonable approach is analyzing the consolidation behavior within homogenization framework.

In this paper, a series of 1-D consolidation tests are performed on sand-marine clay mixtures considering different sand fractions. Correspondingly, a simple consolidation model is proposed and validated using the laboratory data.

Stress (strain) and state variables

The consolidation process is analyzed by dividing the binary mixtures into the marine clay matrix and the sand inclusions (Fig. 2). A marine clay matrix consists of silt particles, clay mineral particles and fluids filling the void space. For simplicity, a representative elementary volume (REV) of the mixture is divided into three parts: the volume of solid part in the clay matrix V_{sc}, including clay mineral particles and silts; the void space in the clay matrix V_v; the volume of sand inclusions V_{ss}. The volume fraction of sand inclusions ϕ_s is given as

$$\phi_s = \frac{V_{ss}}{V_v + V_{sc} + V_{ss}} \tag{1}$$

Since the sand particles are significantly stiffer than the weak clay matrix, they are assumed to be incompressible. The volume of clay matrix decreases with increasing stress level. In this case, ϕ_s is a state variable which increases with the dissipation of excess pore water pressure. It can be computed from the overall porosity of a mixture $n = \frac{V_v}{V_{sc} + V_{ss} + V_v}$ and the local porosity of the clay matrix $n_c = \frac{V_v}{V_{sc} + V_v}$:

$$\phi_s = \frac{n_c - n}{n_c} \tag{2}$$

with the local and overall porosities as

$$n_c = \frac{e_c}{1 + e_c}; \qquad n = \frac{e}{1 + e} \tag{3}$$

where e and e_c are the overall void ratio and the void ratio of the clay matrix, respectively. The void ratios in Eq. (3) are related to the current strains (overall strain ε and local strain ε_c)

and the initial void ratios (overall void ratio e_0 and local void ratio e_{c0}):

$$e = (1 + e_0)\exp(-\varepsilon) - 1; \quad e_c = (1 + e_{c0})\exp(-\varepsilon_c) - 1 \tag{4}$$

Substitution Eqs (3) and (4) into Eq. (2), one computes the stress dependent structure variable ϕ_s. Note that the strains in Eq. (4) are defined as logarithmic strains, and the current vertical strain ε can be calculated from the initial height of a sample and the settlement at an incremental stress level.

Significant difference in stiffness of the constituents leads to a nonuniform stress (strain) distribution (Harshin, 1983; Weng and Tandon, 1988; Kumar, 1996; Shi and Herle, 2017). To this end, the volume average scheme is adopted for the definition of stresses (strains) variables. Assuming a stress field $\boldsymbol{\sigma}'(\boldsymbol{x})$ and a strain field $\boldsymbol{\varepsilon}(\boldsymbol{x})$ within the REV. The overall effective stress and strain are defined as

$$\sigma' = \frac{\int_{V_v+V_{sc}+V_{ss}} \boldsymbol{\sigma}'(\boldsymbol{x})\mathrm{d}V}{V_v + V_{sc} + V_{ss}}; \quad \varepsilon = \frac{\int_{V_v+V_{sc}+V_{ss}} \boldsymbol{\varepsilon}(\boldsymbol{x})\mathrm{d}V}{V_v + V_{sc} + V_{ss}} \tag{5}$$

with σ' and ε denoting the overall effective stress and strain, respectively; Similarly, the local effective stresses (in the clay matrix σ'_c and in the sand σ'_s) and local strain in the clay matrix ε_c can be defined using the volume average scheme.

From the definition of volume groups, one obtains the following relationship between the volume-average stresses (strain) of the constituents and the corresponding overall value:

$$\sigma' = \frac{\int_{V_v+V_{sc}+V_{ss}} \boldsymbol{\sigma}'(\boldsymbol{x})\mathrm{d}V}{V_v + V_{sc} + V_{ss}} = \frac{\int_{V_v+V_{sc}} \boldsymbol{\sigma}'(\boldsymbol{x})\mathrm{d}V + \int_{V_{ss}} \boldsymbol{\sigma}'(\boldsymbol{x})\mathrm{d}V}{V_v + V_{sc} + V_{ss}} = (1 - \phi_s)\sigma'_c + \phi_s\sigma'_s \tag{6a}$$

$$\varepsilon = \frac{\int_{V_v+V_{sc}+V_{ss}} \boldsymbol{\varepsilon}(\boldsymbol{x})\mathrm{d}V}{V_v + V_{sc} + V_{ss}} = \frac{\int_{V_v+V_{sc}} \boldsymbol{\varepsilon}(\boldsymbol{x})\mathrm{d}V}{V_v + V_{sc} + V_{ss}} = (1 - \phi_s)\varepsilon_c \tag{6b}$$

The variables defined above are based on a representative volume element concept. The sand inclusions are assumed to be randomly distributed within the marine clay matrix. Numerical simulations (Tu *et al.*, 2005; Gonzâlez *et al.*, 2004; Shi and Herle, 2017) on this

type of configuration reveal that the REV (contains a statistically sufficient mechanisms) can be well represented by using only a limited number of stiff particles.

Intrinsic behavior of the clay matrix and a homogenization law for sand-clay mixtures

Modelling the compression and permeability of the constituents (marine clay matrix and sand inclusions in this paper) is fundamental for the consolidation analysis of sand-clay mixtures. Since the sand inclusions are incompressible, the overall consolidation process depends on that of the soft marine clay matrix.

Reference model for the pure marine clay

The compression behavior of remolded clays was investigated by many researchers (e.g., Hong *et al.*, 2010; Liu *et al.*, 2013; Shi and Herle, 2015; Zeng *et al.*, 2015; Horpibulsuk *et al.*, 2016). As suggested by Hong *et al.*, (2007), the compression curve of remolded clays can be divided into two distinct regimes: the suction preloading regime below the remolded yield stress σ'_{cy} and the post-yield regime beyond σ'_{cy}. Note that σ'_{cy} is related to the suction stress at the surface of the sample during its preparation. In this study, the remolded yield stress was estimated by extrapolating the post-yield curve to the initial void ratio e_{c0}. As shown in Fig. 3, it is assumed that the deformation is negligible when the stress levels are lower than the remolded yield stress:

$$\ln(1 + e_c) = \ln(1 + e_{c0}) \tag{7}$$

This assumption was introduced for the determination of the remolded yield stress of remolded soils (Hong, 2007, Hong *et al.*, 2010; Shi and Herle, 2016). In this paper, it provides an initial state of the marine clay matrix, which is located on the Normal Compression Line (with a void ratio of e_{c0} at the remolded yield stress σ'_{cy}). In general, the stiffness of the clay matrix is not infinite within the preyield stress range. However, the remolded yield stress of the marine matrix is very low (1.4 kPa). In this case, the above assumption may not lead to

significant error, and such a low stress level is not of interest in many field cases. Furthermore, the difference between the test data and the Normal Compression Line only exists in vicinity of the remolded yield stress, which diminishes with further increase of the consolidation stress level (Fig. 3). In the sequel, the consolidation model is proposed for the normal consolidation range (post-yield stress regime of the clay matrix).

The stiffness of the marine clay matrix shows a sharp decrease in the vicinity of σ'_{cy}, and the compression data beyond the remolded yield stress can be well represented by the compression law proposed by Butterfield (1979):

$$\ln(1 + e_c) = N_c - \lambda_c \ln\sigma'_c \tag{8}$$

Permeability of the pure marine clay

A linear relationship between logarithm of hydraulic conductivity and void ratio was given by Taylor (1948). Subsequent work (Leroueil *et al.*, 1990; Tavenas *et al.*, 1983a and 1983b; Zeng *et al.*, 2011) revealed that the linear e_c-lnk_c relationship was questionable for data with the strain exceeding 20%. To this end, a power relationship between k and e was adopted for the marine clay matrix in this study:

$$\ln k_c = A_c + \xi_c \ln e_c \tag{9}$$

where ξ_c is the slope of the permeability line in a double logarithmic *k:e* plane, and A_c is logarithm of permeability at a reference void ratio e_c=1. This equation was proposed by Mesri and Olson (1971) for the change of permeability during oedometer compression of remolded clays. It was validated by other researchers for various remolded and undisturbed clays (e.g., Somogyi, 1979; Carrier and Beckman, 1984; Pane and Schiffman, 1997, Dolinar, 2009; Zeng *et al.*, 2012).

Homogenization law for sand-clay mixtures

For a binary mixture consists of a soft clay matrix and rigid inclusions, the overall stiffness of a mixture can only increase to several times that of the soft matrix (Hashin, 1983). This postulation was verified by Tu *et al.* (2005) by using Finite Element Method. It indicates that the overall stiffness can be formulated as a function of the local stiffness of the clay matrix. Based on the test data and the analysis of the inter-granular structure, a simple homogenization law was proposed by Shi and Yin (2017) using the tangent stiffness for remolded sand-marine clay mixtures:

$$\ln E = \eta(1 - \phi_s)\ln E_c \tag{10}$$

where E and E_c are the overall tangent stiffness of the mixture and that of the marine clay matrix, respectively; η is a structure variable describing the inter-granular structure evolution, which increases with increasing volume fraction of sand inclusions:

$$\eta = \left(\frac{\tilde{\phi}_s}{\tilde{\phi}_s - \phi_s} \right)^{\beta} \tag{11}$$

where β controls the sensitivity of η on the sand fraction, $\tilde{\phi}_s$ is the maximum volume fraction of the sand inclusions, which is related to the minimum void ratio of the sand skeleton e_{min}:

$$\tilde{\phi}_s = \frac{1}{1 + e_{min}} \tag{12}$$

Governing equations

Based on the volume divisions in Fig. 2, the sand-marine clay mixtures can be divided into two systems: the clay matrix system and the sand inclusion system. The sand inclusion system consists of sand particles V_{ss}, and the clay matrix system is composed of the silts, clay particles and the void space $V_{sc}+V_v$. The deformation of the sand-clay mixtures depends on the constituents (clay matrix and sand inclusions). Since the sand inclusions are

incompressible (Kenney *et al.*, 1992; Mitchell, 1993; Revil *et al.*, 2002), the sand system can be regarded as a closed system (with no fluid and solid exchange with the matrix system). In this case, only the consolidation of the clay matrix system needs to be analyzed.

Conservation of mass

In this study, the continuum principles will be used to derive the balance equations. The procedure follows by coupling the balance equation of masses (including fluid and solid phases within the clay matrix) and Darcy's law. From the definition of clay matrix system, the balance equation of mass to the solid phase in the clay matrix leads to (de Boer and Ehlers, 1986)

$$\frac{\partial \tilde{\rho}_{cs}}{\partial t} + \frac{\partial}{\partial x}\left(\tilde{\rho}_{cs} v_{cs}\right) = \Theta \tag{13}$$

where, Θ is the rate of exchange of solid particles between the clay matrix and the sand inclusions, v_{cs} is the absolute velocity of the solid particles in the clay matrix, If one supposes that no disintegration of the sand particles occurs, the exchange term of vanishes, i.e., $\Theta = 0$. $\tilde{\rho}_{cs}$ denotes the partial density of solid particles in the clay matrix, which is expressed as

$$\tilde{\rho}_{cs} = (1 - \phi_s)(1 - n_c)\rho \tag{14}$$

with ρ denoting the overall density of the sand-clay matrix. It can be computed from the particle densities of the clay matrix ρ_c and the sand inclusions ρ_s. From the conservation of the masses and volumes of the fine and coarse particles before and after mixing process, the overall particle density is deduced as

$$\rho = \frac{\rho_c \rho_s}{\psi_s \rho_c + (1 - \psi_s)\rho_s} \tag{15}$$

Substitution of Eq. (14) into (13) leads to

$$-\frac{\partial}{\partial t}\left[(1 - \phi_s)n_c\right] - \frac{\partial}{\partial x}\left[(1 - \phi_s)n_c v_{cs}\right] + \frac{\partial}{\partial t}(1 - \phi_s) + \frac{\partial}{\partial x}\left[(1 - \phi_s)v_{cs}\right] = 0 \tag{16}$$

202 Applying the same procedure to the fluid phase within the clay matrix, the corresponding
203 conservation of mass can be expressed as

204 $$\frac{\partial}{\partial t}\left[(1-\phi_s)n_c\right]+\frac{\partial}{\partial x}\left[(1-\phi_s)n_c v_{cv}\right]=0 \tag{17}$$

205 where v_{cv} is the absolute velocity of the fluid in the clay matrix. Combining Eq. (16) and (17),
206 the following equation can be obtained:

207 $$\frac{\partial}{\partial x}\left[(1-\phi_s)n_c(v_{cv}-v_{cs})\right]+\frac{\partial}{\partial x}\left[(1-\phi_s)v_{cs}\right]+\frac{\partial}{\partial t}(1-\phi_s)=0 \tag{18}$$

208 A mathematical representation of pore water flow in clay mixtures can be formulated by
209 combining the mass conservation of the solid (Eq. (18)) with Darcy's law. The pore water
210 pressure in the clay matrix is related to the corresponding relative fluid velocity v_r with
211 Darcy's law. Its mathematical description can be written as

212 $$v_r=-\frac{k_c}{\gamma_w}\frac{\partial p_c}{\partial x} \tag{19}$$

213 where p_c is the excess pore water pressure in the clay matrix, γ_w is the unit weight of fluid.
214 Since the sand inclusions are impermeable with no water holding capacity, the local excess
215 pore water pressure p_c is the same as the overall value p of the mixture. The relative fluid
216 velocity (apparent value) v_r in the clay matrix can be expressed as

217 $$v_r=(1-\phi_s)n_c(v_{cv}-v_{cs}) \tag{20}$$

218 Substitution of Eqs (19) and (20) into Eq. (18) gives

219 $$-\frac{k_c}{\gamma_w}\frac{\partial^2 p}{\partial x^2}+(1-\phi_s)\frac{\partial v_{cs}}{\partial x}+v_{cs}\frac{\partial}{\partial x}(1-\phi_s)+\frac{\partial}{\partial t}(1-\phi_s)=0 \tag{21}$$

220 Lagrangian total derivative is introduced in this paper. It includes both the convective rate
221 of change and local rate of change:

222 $$\frac{\mathrm{d}_s}{\mathrm{d}t}(1-\phi_s)=v_{cs}\frac{\partial}{\partial x}(1-\phi_s)+\frac{\partial}{\partial t}(1-\phi_s) \tag{22}$$

Note that in general $v_{cs}\frac{\partial}{\partial x}(1-\phi_s) << \frac{\partial}{\partial t}(1-\phi_s)$ (Valliappan and Khalili-Naghadeh, 1990) for consolidation analysis. Thus, $\frac{\mathrm{d}_s}{\mathrm{d}t}(1-\phi_s) \approx \frac{\partial}{\partial t}(1-\phi_s)$. Eq. (21) can be rewritten as

$$\frac{k_c}{\gamma_w}\frac{\partial^2 p}{\partial x^2} = (1-\phi_s)\frac{\partial v_{cs}}{\partial x} + \frac{\partial}{\partial t}(1-\phi_s) \tag{23}$$

One can see the physical meanings of the items by multiplying Eq. (23) with a unit mass (1 kg). The left side of Eq. (23) denotes mass flow out of the clay matrix; The right side represents the mass change due to volume fraction of the clay matrix (second item) and the corresponding deformation (first item).

Equilibrium equation

Since, the consolidation of sand-marine mixtures is considered as a quasi-static process, the momentum related to the velocity and acceleration of the fluid can be omitted. Hence, the 1D equilibrium equation for sand-clay mixtures is written as

$$\frac{\partial \sigma}{\partial x} + \gamma = 0 \tag{24}$$

Where γ is the unit weight of sand-clay mixtures, and σ is the applied total stress. Note that γ is a state variable which depends on the void ratio:

$$\gamma = \frac{\rho g + e\gamma_w}{1+e} \tag{25}$$

where g is the gravitational acceleration. The local total stress σ is composed of the effective stresses σ' induced by soil particle interactions, and the pore water pressure p in void spaces between soil particles. As state by Graham (1992), the effective stress in a sand-clay mixture is divided into two parts: (1) The net inter-particle unit force σ'_1 between clay particles. It is a combination of various physicochemical forces, e,g., repulsive forces arising from Coulomb repulsion and osmotic forces and attractive forces arising from London-van der Waals forces

between clay particles. (2) physical contacts stress component σ'_2, e.g., the point-point contacts between the sand inclusions. Based on a series of tests on sand-bentonite mixtures, Graham (1992) suggested that the behavior of sand-clay mixtures could be described by effective stresses $\sigma'=\sigma'_1+\sigma'_2$ measured as the difference between pore water pressure p (measured on pressure transducer) and applied total stress σ, i.e., $\sigma'=\sigma-p$. Considering the effective stress concept, the one-dimensional equilibrium equation can be given as

$$\frac{\partial \sigma'}{\partial x}+\frac{\partial p}{\partial x}+\gamma=0 \tag{26}$$

Considering the constitutive relationship Eq. (26) is arranged as

$$E\frac{\partial \varepsilon}{\partial x}+\frac{\partial p}{\partial x}+\gamma=0 \tag{27}$$

with $E=\frac{\mathrm{d}\sigma'}{\mathrm{d}\varepsilon}$ denoting the overall tangent stiffness of sand-marine clay mixtures. The overall vertical strain ε depends on the overall displacement u of the sand-clay mixtures:

$$\varepsilon=-\frac{\partial u}{\partial x} \tag{28}$$

Combining Eqs (27) and (28) yields

$$-E\frac{\partial^2 u}{\partial x^2}+\frac{\partial p}{\partial x}+\gamma=0 \tag{29}$$

The overall stiffness can be derived from the intrinsic compression model of the clay matrix and the homogenization law given in section 2. As mentioned above, the compression curve of the clay matrix can be divided into two distinct regimes. Since no deformation occurs in the clay matrix (Eq. (7)) within the pre-yield regime, the corresponding overall strain increment is negligible. If one supposes that the stress distribution is uniform within the pre-yield stress range, the overall remolded yield stress σ'_y equals the value of the clay matrix, i.e., $\sigma'_y=\sigma'_{cy}$. After the effective stress exceeds the remolded yield stress of the clay matrix, the compression data follow the Normal Compression Line. From the reference compression of

the clay matrix (Eq. (8)), one obtains the corresponding tangent stiffness:

$$E_c = \frac{\mathrm{d}\sigma_c'}{\mathrm{d}\varepsilon_c} = \frac{\sigma_c'}{\lambda_c} \tag{30}$$

Substitution of Eq. (30) into the homogenization law (Eq. (10)), the incremental overall strain of sand-clay mixtures is deduced as

$$\mathrm{d}\varepsilon = \left(\frac{\lambda_c}{\sigma_c'}\right)^{\eta(1-\phi_s)} \mathrm{d}\sigma' \tag{31}$$

Substitution of Eq. (31) into (29) gives

$$-\left(\frac{\lambda_c}{\sigma_c'}\right)^{-\eta(1-\phi_s)} \frac{\partial^2 u}{\partial x^2} + \frac{\partial p}{\partial x} + \gamma = 0 \tag{32}$$

Simplified form of conservation equation

Eqs (23) and (32), are the governing equations for the mass conservation and equilibrium condition, respectively. They are four unknown variants, three volumetric ones (the overall displacement u, the absolute velocity of the soil particles in the clay matrix v_{cs}, the change of the volume fraction of sand inclusions $\frac{\partial \phi_s}{\partial t}$), and the excess pore water pressure p.

Given that the sand inclusions float in the clay matrix, a deformation of the clay matrix induces a rigid displacement of the sand inclusions. Therefore, the absolute velocity of the soil particles in the clay matrix v_{cs}, equals the corresponding velocity of the sand inclusions v_{ss},. The overall velocity of the soil particles of the sand-clay mixture v_s, is given by

$$v_s = (1 - \phi_s)v_{cs} + \phi_s v_{ss} = v_{cs} \tag{33}$$

Note that segregation may happen for sand-clay mixtures with a high initial water content, e.g., 5.0 times the corresponding liquid limit as investigated by previous researchers (Sridharan and Prakash, 1997, 2003; Tan *et al.*, 1990). In this case, the absolute velocity of the sand inclusions is higher than that of the marine clay matrix. However, the initial water

287 content of the tested marine clay matrix is only 1.39 times the corresponding liquid limit, in
288 this case, the segregation can be neglected.

289 Differentiating the overall velocity leads to

290 $$\frac{\partial v_s}{\partial x} = \frac{\partial v_{cs}}{\partial x} = \frac{\partial^2 u}{\partial x \partial t} \tag{34}$$

291 Differentiation of Eq. (1) and considering incompressible sand inclusions, the increment of
292 ϕ_s is given by

293 $$\frac{\partial \phi_s}{\partial t} = \frac{V_t \frac{\partial V_{ss}}{\partial t} - V_{ss} \frac{\partial V_t}{\partial t}}{V_t^2} = -\frac{\phi_s}{V_t} \frac{\partial V_t}{\partial t} \tag{35}$$

294 where V_t=V_v+V_{sc}+V_{ss} is the total volume of the RVE. Considering Eq. (28), Eq. (35) can be
295 rearranged as

296 $$\frac{\partial \phi_s}{\partial t} = \phi_s \frac{\partial \varepsilon}{\partial t} = -\phi_s \frac{\partial^2 u}{\partial x \partial t} \tag{36}$$

297 Substituting Eqs (34) and (36) into Eq. (23) gives

298 $$\frac{k_c}{\gamma_w} \frac{\partial^2 p}{\partial x^2} = \frac{\partial^2 u}{\partial x \partial t} \tag{37}$$

299 *Boundary and initial conditions*

300 The consolidation problem consisting of two governing equations (Eqs (32) and (37)) and
301 two principal variables (overall displacement *u* and excess pore water pressure *p*) need to be
302 solved in a predefined domain. The boundary and initial conditions for the problem should be
303 defined. Supposing that there are three boundaries, Γ1, Γ2 and Γ3, corresponding to the
304 overall displacement, pore pressure and fluid flow, respectively. Note that the above partial
305 boundaries give a full boundary of the consolidation problem Γ, i.e., Γ=Γ1∪Γ2∪Γ3.
306 Correspondingly, the boundary conditions are expressed as

307 $$u(x,t) = \bar{u}(x,t);\ x \in \Gamma 1, t \in [0, \infty) \tag{38}$$

$$p(x,t) = \bar{p}(x,t);\ x \in \Gamma 2, t \in [0,\infty) \tag{39}$$

$$k_c \frac{\partial p(x,t)}{\partial t} = \bar{q}(x,t);\ x \in \Gamma 3, t \in [0,\infty) \tag{40}$$

where $\bar{u}(x,t)$, $\bar{q}(x,t)$ and $\bar{p}(x,t)$ are overall displacement, fluid flow and pore pressure on the boundaries Γ1, Γ2 and Γ3 respectively. The initial pore water distribution on the complete boundary is given as

$$p(x,0) = \bar{p}_0(x);\ \ x \in \Gamma \tag{41}$$

Combining Eqs (32), (37)-(41), the consolidation problem can be solved using Galerkin's weighted residuals method within the finite element concept. The solving procedures have been documented by many researchers for its application to consolidation analysis (e.g., Khaled *et al.*, 1984; Valliappan *et al.*, 1990), which will be not given in details in this study.

Model evaluation

Analysis of the experimental data

For producing sand-clay mixtures, a coarse sand material (sand inclusions) and a soft clayey soil (clay matrix) from Hong Kong Marine Deposits were used. The basic physical properties of the two materials are given in Table 1 (according to BS1377). The sand material has a minimum void ratio of 0.601 and a maximum one of 0.945, respectively. Water was added to the marine clay to reach a water content of 86.9%. Then, it was mixed with the sands homogeneously with various sand fractions (0%, 20%, 40%, 60%). The samples were consolidated at an initial stress of 1.7 kPa, then increased stepwise, from 2.5 kPa to 800 kPa. For a given stress increment, the settlement of the sample was recorded up to the end of primary consolidation. The saturation ratio defined as the ratio of the measured initial water content to the corresponding theoretical value (estimated by assuming a saturated condition) is higher than 0.98. For more details of producing the sand-marine clay mixtures, one can

refer to Shi and Yin (2017).

Fig. 4 shows the consolidation behavior of the sand-marine clay mixtures in terms of time duration and degree of consolidation in semi-logarithmic plot. The consolidation curves with different sand fractions show similar trend: the degree of consolidation increases with increasing applied total stress at the same consolidation time, indicating a rapider dissipation of the excess pore water pressure due to the decreasing thickness of the samples. The influence of sand fraction on the consolidation behavior is shown in Fig. 5. It is seen that the consolidation curve of the mixtures with a sand fraction of 20% is approximately close to that of the pure marine clay. However, further increase of the sand fraction accelerates the consolidation process. This phenomenon can be explained by the local stress distribution in sand-clay mixtures, which is characterized by an incremental stress ratio μ_σ^c, defined as

$$\mu_\sigma^c = \frac{\mathrm{d}\sigma_c'}{\mathrm{d}\sigma'} \tag{42}$$

From Eqs (6), (30) and (31), the stress ratio is derived:

$$\mu_\sigma^c = (1-\phi_s)^{-1}\left(\frac{\sigma_c'}{\lambda_c}\right)^{1-\eta(1-\phi_s)} \tag{43}$$

Since the local stress in the clay matrix is lower than that in the sand inclusions, the consolidation behavior of sand-clay mixtures is different from that of the corresponding clay matrix. It is seen from Eq. (43) that the stress distribution is controlled by two variables, the volume fraction of the sand particles ϕ_s and the structure parameter η.

For the tested sand-marine clay mixture with a sand mass fraction of 20%, the volume fraction of the sand inclusions is close to 0.1 and the structure parameter η is approximately close to 1 (Fig. 7), which means that the local stress in the clay matrix is relatively close to the corresponding overall value (referring to Eq. (43)). Consequently, the corresponding consolidation curve nearly overlap with that of the pure clay sample at the same surcharge loading. However, the stress ratio decreases remarkably with further increase of sand fraction

(20% and 40% in this study), leading to a higher void ratio (Eq. (8)) and a higher permeability (Eq. (9)) of the clay mixtures.

The influence of sand mass fraction on the consolidation behavior of sand-clay mixtures depends on the clay minerals in the clay matrix. For the sand-clay mixtures with a clay matrix consisting of Nontronite or Kaolinite, the volume fraction may be much higher than 0.1 for a sand mass fraction of 20% and an initial water content of the clay matrix of $1.39w_L$. In this case, the stress distribution becomes less uniform, and the overall consolidation behavior may be much more different from that of the pure clay matrix. However, for the sand-clay mixtures with bentonite matrix, the liquid limit of the matrix may be as high as 600%. Consequently, even 50% sand mass fraction may not significantly affect the consolidation of the clay matrix in the mixtures (the corresponding initial volume fraction of the sand inclusions is relatively low due to the relatively high initial water content of the clay matrix).

Model parameters and calibration

There are five principal parameters for the consolidation model: A_c, ξ_c, N_c, λ_c and β. The first four parameters correspond to the intrinsic behavior of the clay matrix. A_c and ξ_c are permeability parameters of the clay matrix, which can be calibrated from permeability data of the pure clay; N_c and λ_c are intrinsic compression parameters of the clay matrix corresponding to the Normal Compression Line of the pure clay. β is a structure parameter related to the inter-granular structure evolution. It is suggested to calibrate this parameter from permeability data of a sand-clay mixture with a predefined sand fraction. Therefore, one needs to do at least two 1-D consolidation tests: one on the pure clay to estimate the intrinsic model parameters, and one on the sand-clay mixture for calibrating the structure parameter.

The permeability of the pure marine clay can be computed according to the corresponding compressibility and consolidation curves (from the definition of coefficient of consolidation):

$$k_c = \frac{\delta\varepsilon_c c_v \lambda_w}{\delta\sigma'_c} \tag{44}$$

where $\delta\varepsilon_c$ is the strain increment for a given effective stress increment $\delta\sigma'_c$, C_v=0.212h^2/t_{90}, t_{90} is the time period corresponding to 90% of consolidation, which can be determined from the corresponding consolidation data, and h is the height of the sample. The computed data for the pure marine clay are shown in Fig. 6 in terms of permeability and void ratio on a double-logarithmic scale. It is seen that there is a good linear relationship between ln$k$ and ln$e$, which is consistent with Eq. (9). The model parameters are calibrated as shown in Fig. 6 and Fig. 8 (referring to Eq. (8), the compression data in Fig.8 are from Shi and Yin (2017)). β was calibrated by trial and error method (Fig. 7). The model parameters are given in Table 1. It can be seen from Fig. 8 that the compression data of the sand-marine clay mixtures can be well reproduced by the compression model (Eqs (2)-(4), (11), (30), (31) and (43)).

Evaluation of the model

The consolidation data below 10 kPa are not included in the model evaluation, since the measurements may be not reliable at such small stress levels. The samples have a thickness of 1.9 cm. Both the bottom and top surfaces of the samples are free draining, and the bottom surface was fixed during the consolidation process. The boundary conditions in section 4.4 (Eqs (38) - (40)) are:

$$p(0, t) = 0; \sigma(0, t) = \sigma_n \tag{45}$$

$$u(1.9, t) = 0; \; p(1.9, t) = 0 \tag{46}$$

where σ_n is total stress corresponding to the load on the top surface of the samples. The mixture samples are supposed to have an uniform initial stress, with an effective stress of 1.4 kPa (corresponding to remolded yield stress of the marine clay matrix), $\sigma'_c(x,0)=\sigma'_s(x,0)$=1.4 kPa. The initial void ratio of the marine clay matrix is 2.33. The overall void ratios of the samples are 1.84, 1.36 and 0.89, corresponding to the sand fractions of 20%, 40% and 60%,

403 respectively.

404 A three-nodes bar element is used in this study (see Fig. 9, δh denotes the element size),
405 which gives a linear variation of pore pressure and a quadratic variation of displacement. The
406 model was discretized with 20 elements and a surcharge load of 3.6 kPa was applied on the
407 top surface. Subsequent load was applied stepwise following steps of 5, 10, 25, 50, 100, 200,
408 400 and 800 kPa.

409 The consolidation tests of the sand-marine clay mixtures were simulated using the model
410 parameters listed in Table 1. The predicted consolidation curves at different stress levels are
411 shown in Fig. 10 together with the experimental data. It can be seen that the effect of sand
412 fraction on the consolidation behavior of the sand-marine clay mixtures can be well
413 reproduced by the proposed model: for a given consolidation time, the degree of consolidation
414 increases with increasing sand fraction. The prediction curves are approximately close to the
415 laboratory results for sand fractions of 20% and 40%. However, there is a slight difference
416 between the test data and model simulations for a sand fraction of 60%. This may be
417 explained by the inter-granular structure. Although the volume fraction of the sand inclusions
418 (ψ_s= 60%) is lower than the minimum value $\tilde{\phi}_s$, there may be possibly direct contacts between
419 the sand inclusions, which induces partial force chains in the mixture. However, the contacts
420 and force chains are not stable, and the inter-granular structure would rearrange and adjust
421 itself to a new effective stress state. As a result, the stress is gradually transferred from the
422 sand inclusions to the clay matrix, which would slow the consolidation process of the clay
423 matrix.

424 **Conclusions**

425 In this paper, the consolidation behavior of saturated sand-clay mixtures is modelled within
426 homogenization framework. Capability of the model is evaluated based on the laboratory tests

on the remolded sand-marine clay mixtures. Based on the data analysis and validation of the proposed model, the following conclusions are drawn:

(1) The consolidation curve of the sand-marine with a sand fraction of 20% is approximately close to that of the pure marine clay. Further increase of the sand fraction significantly accelerates the consolidation process. This is due to a remarkable decrease of the local stress in the clay matrix with increasing sand fraction, which induces a higher void ratio and a higher permeability of the clay matrix.

(2) As a binary material, the sand-marine clay mixture is divided into two systems: the matrix system consisting of the silts, void space and clay particles in the marine clay matrix, and the sand inclusion system consisting of sand material. Two governing equations, the mass of conservation equation and the equilibrium equation, are derived based on a few reasonable assumptions.

(3) The proposed consolidation model has five principal parameters, four intrinsic ones depending on the behavior of the pure marine clay matrix, and one structure parameter related to the inter-granular structure evolution. The parameters can be easily calibrated based on two conventional consolidation tests.

(4) Comparison between the test data and the model prediction reveals that the model can well reproduce the consolidation behavior of the tested sand-marine clay mixtures. A slight overestimation of the degree of consolidation with a sand fraction of 60% may be induced by possible contacts and force chains of the sand inclusions.

As presented in the text, several basic assumptions are adopted, which limits the application of the proposed consolidation model:

(1) It is assumed that no deformation of the clay matrix occurs within the pre-yield stress range. This assumption is used for estimating the remolded yield stress σ'_{cy} of the marine clay

matrix (see Fig. 3) and provides an initial state for the consolidation analysis. There may be some difference between the model prediction and the test data at very small stress levels, e.g., in vicinity of the remolded yield stress of the clay matrix (σ'_{cy} =1.4 kPa for Hong Kong marine clay). However, in many field cases, such a low stress level is not of interest.

(2) It is assumed that the absolute velocity of the soil particles in the clay matrix equals the corresponding velocity of the sand inclusions. The proposed model is not suitable for the clay matrix with a relatively high initial water content, which shows segregation during the compression tests. (Sridharan and Prakash, 1997, 2003; Tan *et al.*, 1990).

Acknowledgements

The work in this paper is supported by a National State Key Project "973" grant (Grant No.: 2014CB047000) (sub-project No. 2014CB047001) from Ministry of Science and Technology of the People's Republic of China, a CRF project (Grant No.: PolyU12/CRF/13E) from Research Grants Council (RGC) of Hong Kong Special Administrative Region Government of China. The authors acknowledge also the financial supports from Research Institute for Sustainable Urban Development of The Hong Kong Polytechnic University.

References

British Standards Institution (1991). Methods of test for soils for civil engineering purposes, *BS 1377*. BSI, Milton Keynes.

Butterfield, R. (1979). A natural compression law for soils (an advance on *e*-log*p*′). *Géotechnique*, 29(4).

Carrier, W. D., & Beckman, J. F. (1984). Correlations between index tests and the properties of remoulded clays. *Géotechnique*, 34(2), 211-228.

de Boer, R., & Ehlers, W. (1986). On the problem of fluid-and gas-filled elasto-plastic solids. *International journal of solids and structures*, 22(11), 1231-1242.

Deng, Y., Wu, Z., Cui, Y., Liu, S., & Wang, Q. (2017). Sand fraction effect on hydro-mechanical behavior of sand-clay mixture. *Applied Clay Science*, 135, 355-361.

de Magistris, F. S., Silvestri, F., & Vinale, F. (1998). Physical and mechanical properties of a compacted silty sand with low bentonite fraction. *Canadian Geotechnical Journal*, 35(6), 909-925.

Dolinar, B. (2009). Predicting the hydraulic conductivity of saturated clays using plasticity-value correlations. *Applied Clay Science*, 45(1), 90-94.

Elkady, T. Y., Shaker, A. A., & Dhowain, A. W. (2015). Shear strengths and volume changes of sand-attapulgite clay mixtures. *Bulletin of Engineering Geology and the Environment*, 74(2), 595-609.

González, C., Segurado, J., & LLorca, J. (2004). Numerical simulation of elasto-plastic deformation of composites: evolution of stress microfields and implications for

502 homogenization models. *Journal of the Mechanics and Physics of Solids*, 52(7), 1573-1593.
503 Graham, J., Oswell, J. M., & Gray, M. N. (1992). The effective stress concept in saturated
504 sand-clay buffer. *Canadian Geotechnical Journal*, 29(6), 1033-1043.
505 Hashin, Z. (1983). Analysis of composite materials. *Journal of Applied Mechanics*, 50(2),
506 481-505.
507 Hong, Z. (2007). Void Ratio-Suction Behavior of Remolded Ariake Clays. *Geotechnical*
508 *Testing Journal*, 30(3), 234-239.
509 Hong, Z., Yin, J., & Cui, Y. J. (2010). Compression behavior of reconstituted soils at high
510 initial water contents. *Géotechnique*, 60(9), 691-700.
511 Horpibulsuk, S., Liu, M. D., Zhuang, Z., & Hong, Z. S. (2016). Complete compression curves
512 of reconstituted clays. *International Journal of Geomechanics*, 16(6).
513 Kenney, T. C., Veen, W. V., Swallow, M. A., & Sungaila, M. A. (1992). Hydraulic
514 conductivity of compacted bentonite-sand mixtures. *Canadian Geotechnical Journal*, 29(3),
515 364-374.
516 Khaled, M. Y., Beskos, D. E., & Aifantis, E. C. (1984). On the theory of consolidation with
517 double porosity-3 A finite element formulation. *International journal for numerical and*
518 *analytical methods in geomechanics*, 8(2), 101-123.
519 Kumar, G. V. (1996). Some aspects of the mechanical behavior of mixtures of kaolin and
520 coarse sand (*Doctoral dissertation, University of Glasgow*).
521 Leroueil, S., Bouclin, G., Tavenas, F., Bergeron, L., & Rochelle, P. L. (1990). Permeability
522 anisotropy of natural clays as a function of strain. *Canadian Geotechnical Journal*, 27(5),
523 568-579.
524 Liu, M. D., Zhuang, Z., & Horpibulsuk, S. (2013). Estimation of the compression behavior of
525 reconstituted clays. *Engineering Geology*, 167, 84-94.
526 Mesri, G., & Olson, R. E. (1971). Mechanisms controlling the permeability of clays. *Clays*

527 *and Clay Minerals*, 19(1), 151-158.
528 Mitchell, J. K. 1993, Fundamentals of Soil Behavior, *John Wiley and Sons*, Inc., New York.
529 Monkul, M. M., & Ozden, G. (2005). Effect of intergranular void ratio on one-dimensional
530 compression behavior. In *Proceedings of International Conference on Problematic Soils*,
531 International Society of Soil Mechanics and Geotechnical Engineering, Famagusta, Turkish
532 Republic of Northern Cyprus (Vol. 3, pp. 1203-1209).
533 Monkul, M. M., & Ozden, G. (2007). Compressional behavior of clayey sand and transition
534 fines content. *Engineering Geology*, 89(3), 195-205.
535 Pane, V., & Schiffman, R. L. (1997). The permeability of clay suspensions. *Géotechnique*,
536 47(2), 273-288.
537 Pandian, N. S., Nagaraj, T. S., & Raju, P. N. (1995). Permeability and compressibility
538 behavior of bentonite-sand/soil mixes. *Geotechnical Testing Journal*, 18(1) ,86-93.
539 Pusch, R., & Gray, M. (1989). Sealing of radioactive waste repositories in crystalline rock. *In*
540 *Sealing of Radioactive Waste Repositories*.
541 Revil, A., Grauls, D., & Brévart, O. (2002). Mechanical compaction of sand/clay mixtures.
542 *Journal of Geophysical Research: Solid Earth*, 107(B11).
543 Shi, X. S., & Herle, I. (2015). Compression and undrained shear strength of remoulded clay
544 mixtures. *Géotechnique Letters*, 5(2), 62-67.
545 Shi, X. S., & Herle, I. (2016). Modeling the compression behavior of remolded clay mixtures.
546 *Computers and Geotechnics*, 80, 215-225.
547 Shi, X. S. and Herle, I. (2017). Numerical simulation of lumpy soils using a hypoplastic
548 model. *Acta Geotechnica* 12, 349-363
549 Shi X. S., & Yin, J. H. (2017). Experimental and theoretical investigation on remolded sand-
550 marine clay mixtures within homogenization framework. (submitted).
551 Silva, S. D. Three runway system project (3RS project), contract 3206 – main reclamation

552 works. *Report for ZHECC-CCCC-CDC joint venture*. 7076481/R00: Hong Kong, 2016.
553 Sivapullaiah, P. V., Sridharan, A., & Stalin, V. K. (2000). Hydraulic conductivity of
554 bentonite-sand mixtures. *Canadian Geotechnical Journal*, 37(2), 406-413.
555 Somogyi, F. (1979). Analysis and prediction of phosphatic clay consolidation:
556 implementation package. Lakeland: *Florida Phosphatic Clay Research Project* (Technical
557 Report).
558 Sridharan, A and Prakash, K. (1997). Settling Behavior of Fine Grained Soils. *Indian*
559 *Geotechnical Journal*, 27(3), 278-309.
560 Sridharan, A. and Praksh，K. (2003). SelfWeight Consolidation: Compressibility Behavior of
561 Segregated and Homogeneous Finegrained Sediments. *Marine Georesources and*
562 *Geotechnology*, 21, 73-80.
563 Tan, S. A., Karunaratne, G. P., & Muhammad, N. (1994). Sand penetration into clay slurry
564 through jute interlayer. *Soils and foundations*, 34(2), 19-25.
565 Tan, T. S., Yong, K. Y., Leong, E. C., Lee, S. L. (1990). Behavior of clay slurry. *Soils and*
566 *Foundations*, 30(4), 105-118.
567 Tavenas, F., Leblond, P., Jean, P., & Leroueil, S. (1983). The permeability of natural soft
568 clays. Part 1: Methods of laboratory measurement. *Canadian Geotechnical Journal*, 20(4),
569 629-644.
570 Tavenas, F., Jean, P., Leblond, P., & Leroueil, S. (1983). The permeability of natural soft
571 clays. Part 2: Permeability characteristics. *Canadian Geotechnical Journal*, 20(4), 645-660.
572 Taylor, D. W. (1948). Fundamentals of soil mechanics. *LWW*.
573 Torfs, H., Mitchener, H., Huysentruyt, H., & Toorman, E. (1996). Settling and consolidation
574 of mud/sand mixtures. *Coastal Engineering*, 29(1-2), 27-45.
575 Tu, S. T., Cai, W. Z., Yin, Y., & Ling, X. (2005). Numerical simulation of saturation behavior
576 of physical properties in composites with randomly distributed second-phase. *Journal of*

composite materials, 39(7), 617-631.

Valliappan, S., & Khalili-Naghadeh, N. (1990). Flow through fissured porous media with deformable matrix. *International journal for numerical methods in engineering*, 29(5), 1079-1094.

Watabe, Y., Yamada, K., & Saitoh, K. (2011). Hydraulic conductivity and compressibility of mixtures of Nagoya clay with sand or bentonite. *Géotechnique*, 61(3), 211-219.

Weng, G. J., & Tandon, G. P. (1988). A theory of particle-reinforced plasticity. *ASME Journal of Applied Mechanics*, 55(3), 126-135.

Yin, J. H. (1999). Properties and behavior of Hong Kong marine deposits with different clay contents. *Canadian Geotechnical Journal*, 36(6), 1085-1095.

Zeng, L. L., Hong, Z. S., & Chen, F. Q. (2012). A law of change in permeability coefficient during compression of remolded clays. *Rock and Soil Mechanics*, 5, 001.

Zeng, L. L., Hong, Z. S., Cai, Y. Q., & Han, J. (2011). Change of hydraulic conductivity during compression of undisturbed and remolded clays. *Applied Clay Science*, 51(1), 86-93.

Zeng, L. L., Hong, Z. S., & Cui, Y. J. (2015). Determining the virgin compression lines of reconstituted clays at different initial water contents. *Canadian Geotechnical Journal*, 52(9), 1408-1415.

602

603

604

605

606

607

Table 1: Basic physical properties of the tested materials

Materials ---	Liquid Limit (%)	Plastic Limit (%)	Density of particles (Mg/m^3)	Clay (%)	Silt (%)	Sand (%)
Sand	---	---	2.63	0	0	100
Clay	62.4	27.5	2.68	15	85	0

Table 2: Model parameters of the consolidation model for sand-marine clay mixtures

A_c	ξ_c	N_c	λ_c	β
m/s	*m/s*	---	---	---
-22.73	4.15	1.24	0.10	0.75

List of Figures

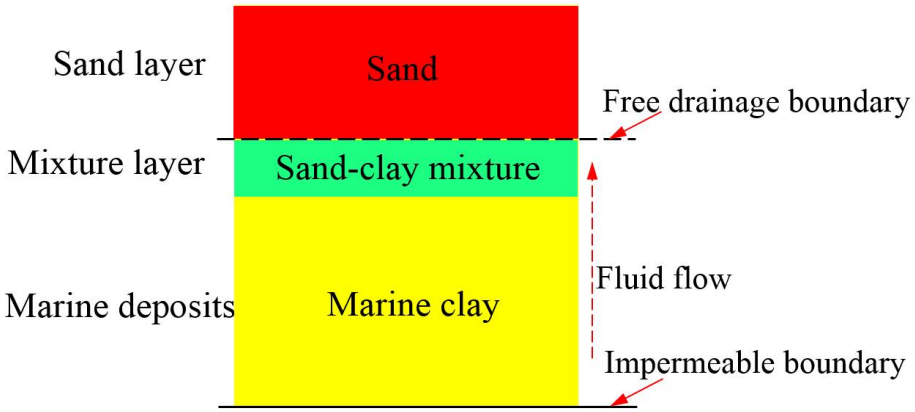

Figure 1: Schemetric profile of soil layers in a marine reclamation physical model

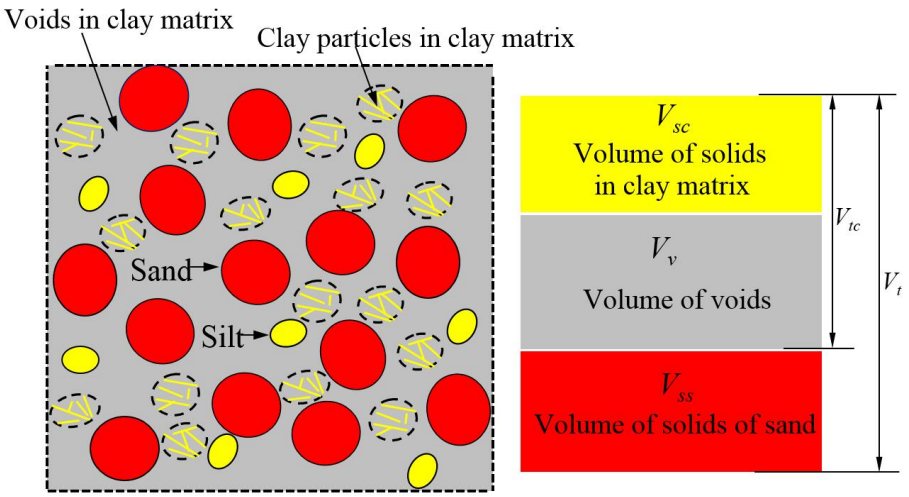

Figure 2: Volume divisions for RVE of remolded sand-clay mixtures (from Shi and Yin, 2017)

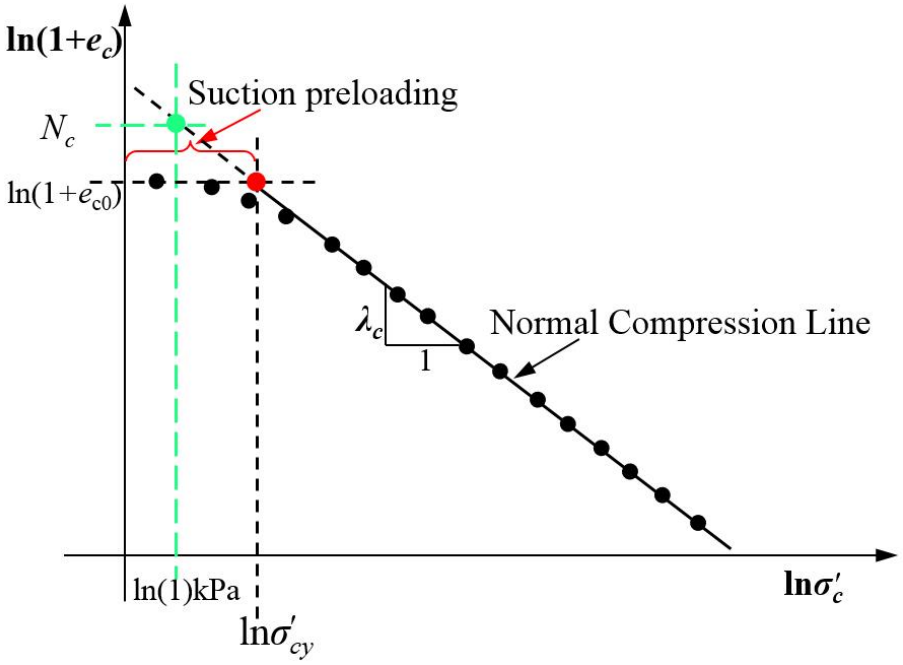

Figure 3: Schemetric plot for the compression model of the pure marine clay

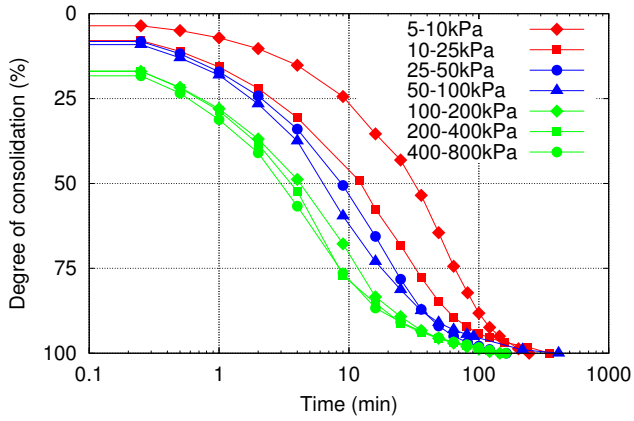

(a) ψ=0 %

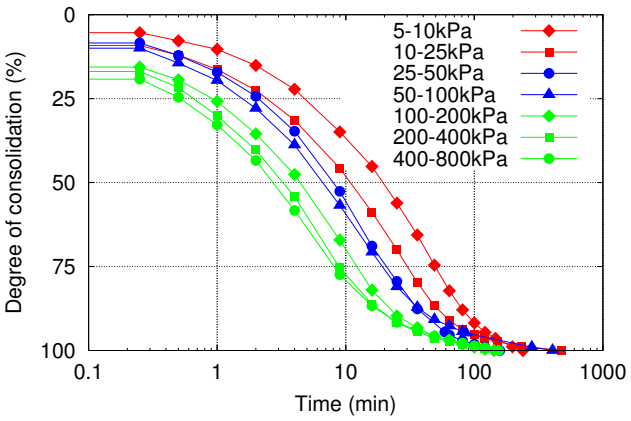

(b) ψ=20 %

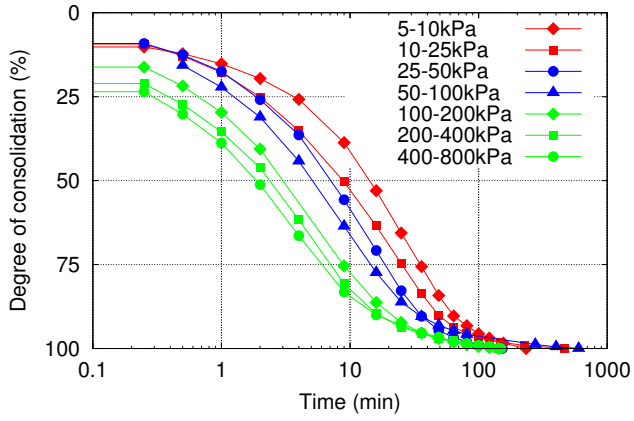

(c) ψ=40 %

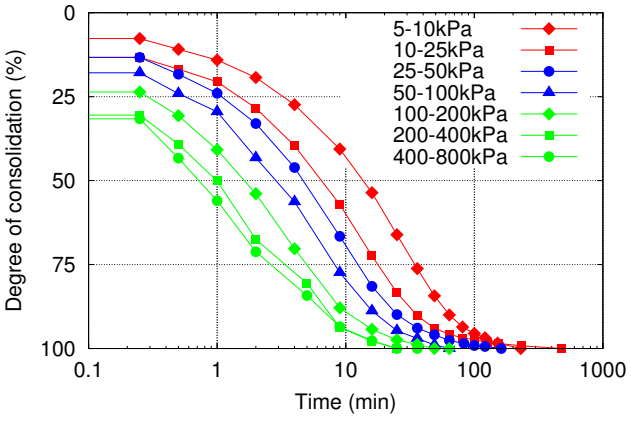

(d) ψ=60 %

Figure 4: Consolidation curves of sand-marine clay mixtures with different sand fractions

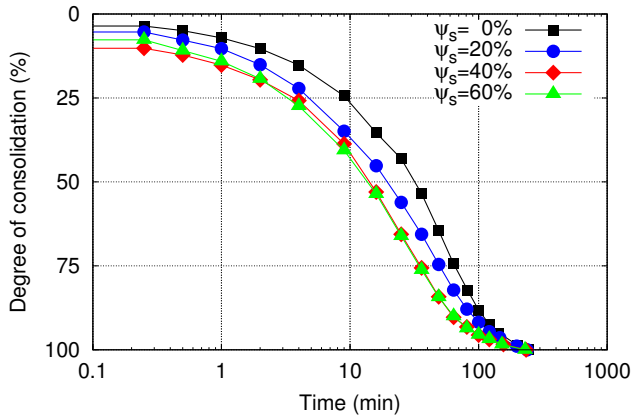

(a) σ=10 kPa

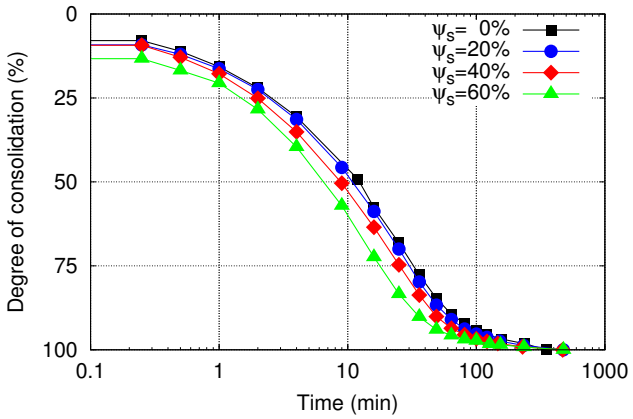

(b) σ=25 kPa

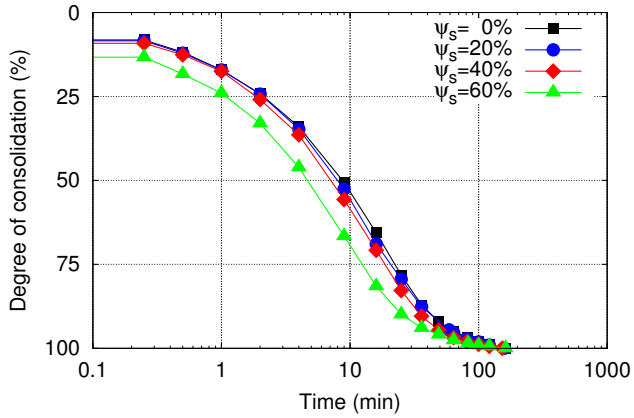

(c) σ=50 kPa

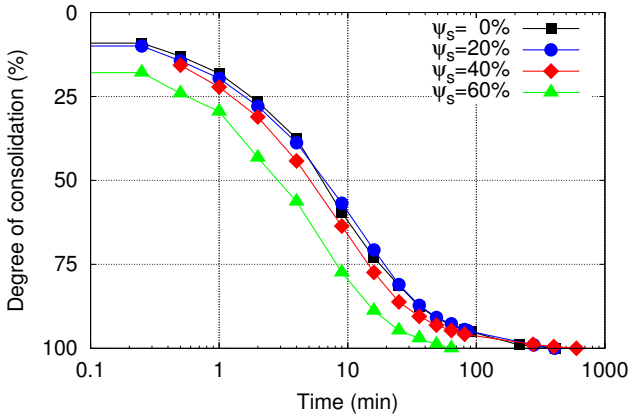

(d) σ=100 kPa

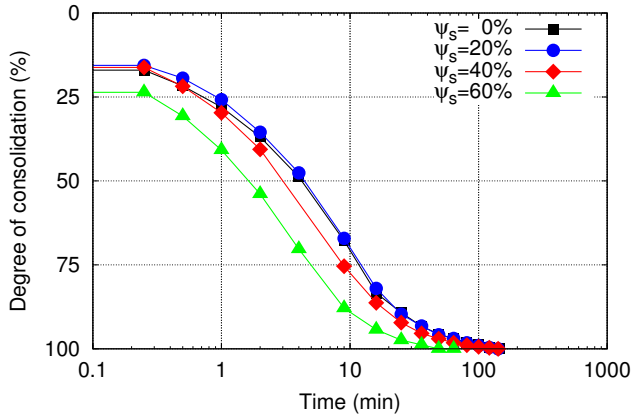

(e) σ=200 kPa

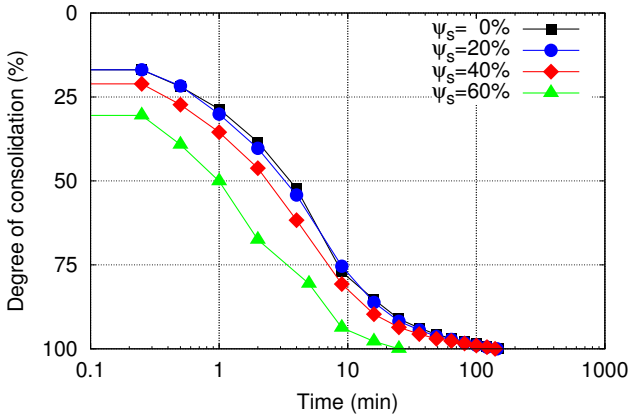

(f) σ=400 kPa

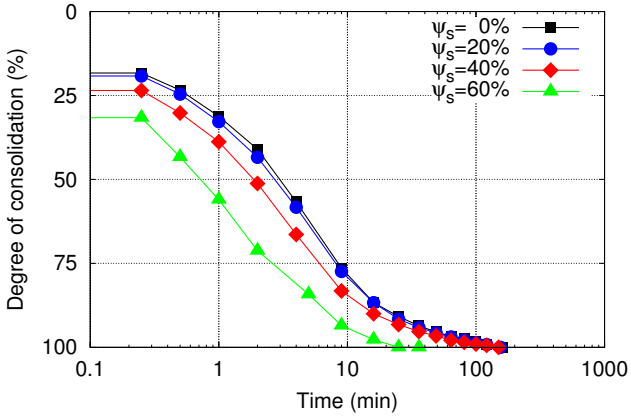

(g) σ=800 kPa

Figure 5: Consolidation curves of sand-marine clay mixtures at different stress levels

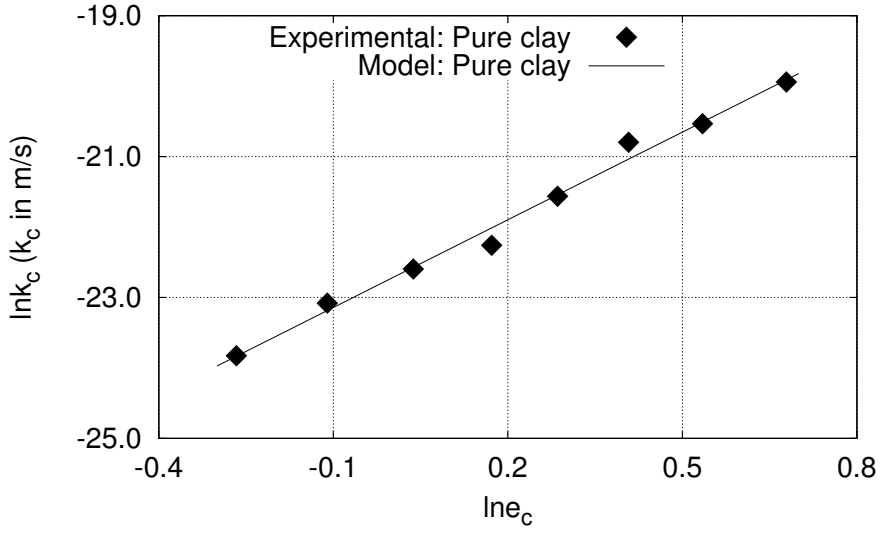

Figure 6: Calibration of intrinsic permeability parameters of pure marine clay

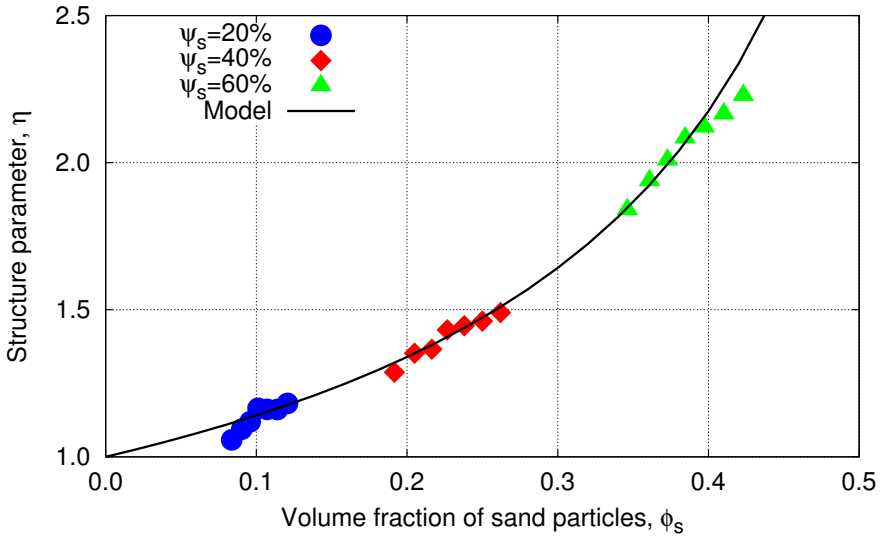

Figure 7: Calibration of structure parameter of sand-marine clay mixtures

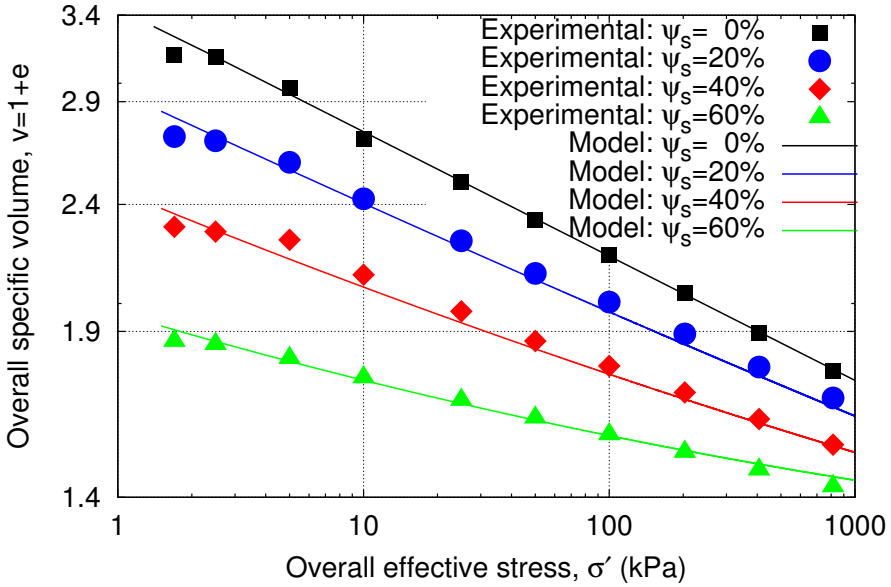

Figure 8: Calibration of intrinsic compression parameters of sand-marine clay mixtures

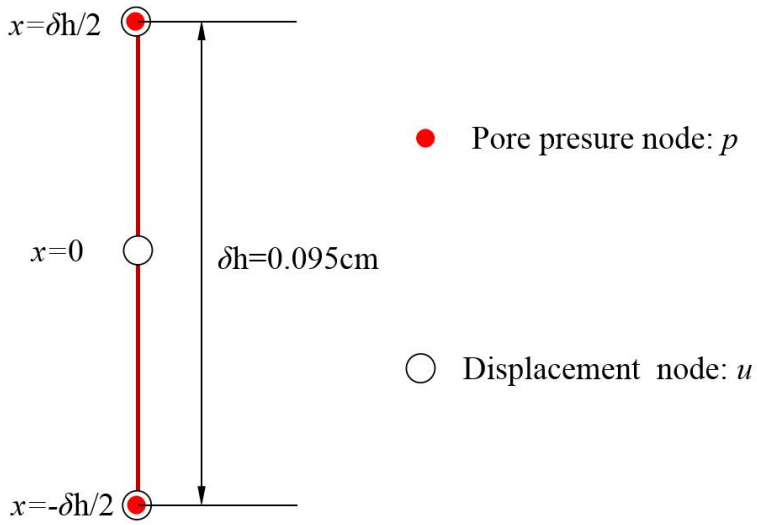

Figure 9: Finite element used for the 1-D consolidation analysis for sand-marine clay mixtures

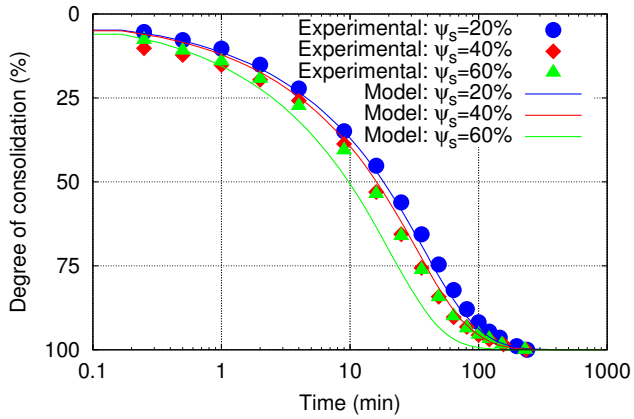

(a) σ=10 kPa

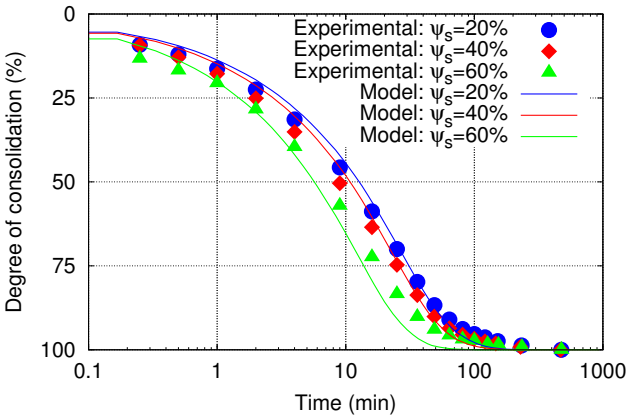

(b) σ=25 kPa

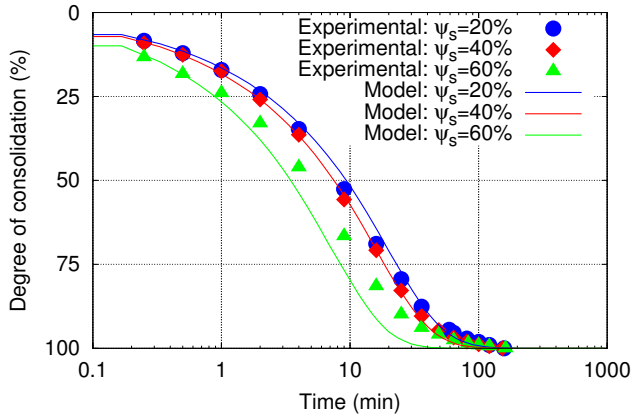

(c) σ=50 kPa

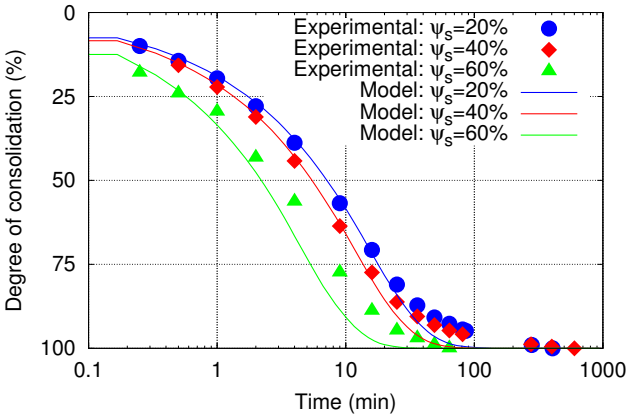

(d) σ=100 kPa

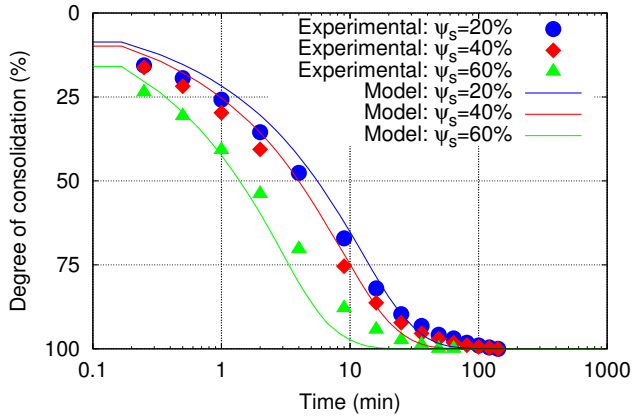

(e) σ=200 kPa

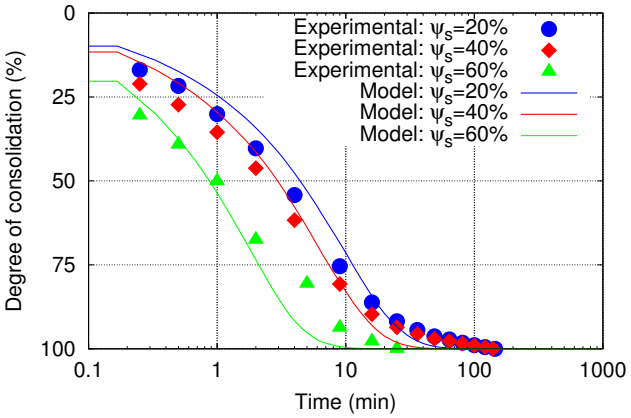

(f) σ=400 kPa

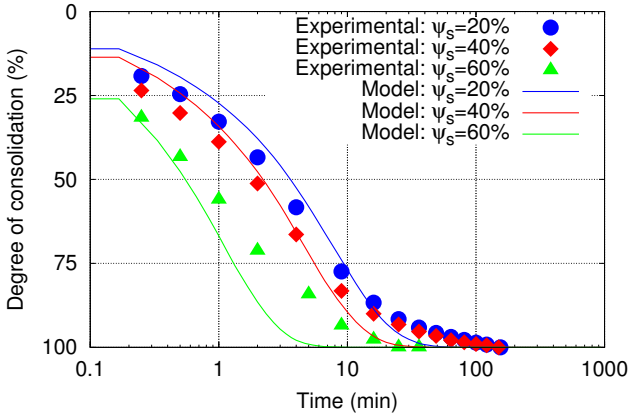

(g) σ=800 kPa

Figure 10: Comparison between the test data and simulated consolidation curves